Food and Bioprocess Technology (2020) 13:827–837
https://doi.org/10.1007/s11947-020-02438-5

ORIGINAL PAPER

Cold Atmospheric Plasma Inactivation of Microbial Spores Compared on Reference Surfaces and Powder Particles

Michael Beyrer[1] · Irina Smeu[1,2] · David Martinet[3] · Alan Howling[4] · Maria Consuelo Pina-Pérez[1] · Christoph Ellert[3]

Received: 28 March 2019 / Accepted: 4 April 2020 / Published online: 18 April 2020

Abstract

Heat-resistant spores on a dry, heat- and water-sensitive food matrix are difficult to inactivate. Radioactive or X-ray exposure is allowed and accepted only for some selected commodities. Non-thermal atmospheric pressure plasma treatments could offer an efficient, fast, and chemical-free solution. The effectiveness of direct contact cold atmospheric plasma (CAP) generated by a dielectric barrier discharge (DBD) device and air as process gas was evaluated against spores of *Bacillus* spp., *Geobacillus* spp., and *Penicillium* spp. A maximum of 3 $\log_{10}$ cycles of inactivation was achieved for *B. coagulans* spores exposed for only 10 s at low surface energy of 0.18 W/cm^2 determined directly at the electrodes. This corresponds to an initial decimal reduction time of $D_1 = 0.1$ min. Spores of *B. subtilis* are the most resistant amongst the studied strains ($D_1 = 1.4$ min). The determining parameter in the modeling of the inactivation curve is surface energy. Non-porous, native starch granules or shells from diatoms, a highly porous material, were also contaminated with spores and treated by DBD CAP. The inactivation level was significantly reduced by the presence of powders. Considering plasma diagnostics, it can be concluded that the spore shell is the primary and main target for a plasma-induced inactivation. The inactivation affect scales with surface energy and can be controlled directly via process time and/or discharge power.

Keywords Direct atmospheric plasma · Dielectric barrier discharge · Spores · Inactivation kinetics

Introduction

Several outbreaks of food-borne diseases have been attributed to powdered food (CDC 2014; Cheon et al. 2015). The decontamination of powdered food remains a challenge because the application of dry or wet heat is limited, and non-thermal processing options such as high hydrostatic pressure (HHP) or pulsed electric fields (PEFs) apply to liquids only. Amongst the emerging sanitizing and preservation technologies, vacuum-steam-vacuum processing (Hörmannsperger et al. 2016; Kozempel et al. 2002), e-beam (Jung et al. 2015), and cold atmospheric plasma (CAP) treatment (Hertwig et al. 2015a; Kim et al. 2014) have an underdeveloped potential in decontamination of food powders.

Up to date, plasma technology has been demonstrated to be effective in the treatment of superficially contaminated fresh food by killing mainly vegetative living cells of pathogenic bacteria (Mitra et al. 2014; Misra et al. 2014; Wang et al. 2016a) or even in liquid media (Gurol et al. 2012). In addition, some studies are focused on the inactivation of microbial spores (Hertwig et al. 2017; Wang et al. 2016b).

Spores, the dormant form of some microorganisms, and specifically bacterial endospores, are considered to be the most resistant to inactivation using conventional physical treatments (e.g., dry heat, irradiation, UV, high pressure) and chemical agents (e.g., hydrogen peroxide) (Kelly-Wintenberg et al. 1999). Spores have durable coat layers, which make them resistant to conventional thermal sterilization methods (Muranyi et al. 2008; Setlow 2006), and suitable for benchmarking novel sanitizing methods (Black et al. 2007).

✉ Michael Beyrer
michael.beyrer@hevs.ch

[1] Institute of Life Technologies, University of Applied Sciences Western Switzerland (HES-SO Valais-Wallis), 64 Route du Rawyl, 1950 Sion 2, Switzerland

[2] National R&D Institute for Food Bioresources–IBA Bucharest, 6 Dinu Vintila Street, 2nd District, 021102 Bucharest, Romania

[3] Institute of Systems Engineering, University of Applied Sciences Western Switzerland (HES-SO Valais-Wallis), 47 Route du Rawyl, 1950 Sion, Switzerland

[4] Swiss Plasma Center, Ecole Polytechnique Fédérale de Lausanne (EPFL), 1015 Lausanne, Switzerland

Process gases such as air, nitrogen, and oxygen, or noble gases such as argon and helium, can be used for plasma treatment (Misra et al. 2014). When adding electrical energy to the system, the components of the gas break down and the gas becomes excited, ionized, and dissociated, thus forming a plasma. Free radicals, charged particles, photons, and UV radiation inactivate living microorganisms or cells in tissues by various mechanisms, owing to the complexity of both the plasma and the cells (Dobrynin et al. 2009).

Besides the gas layer itself, the main barriers protecting the DNA in spores are the electron-dense outer layer and a lamella-like inner coating. According to the studies of Riesenman and Nicholson (2000), the shielding efficiency depends strongly on the bacterial strain for *Bacillus subtilis* and appears to be attributable to genetically defined differences.

In addition, reactive oxygen species (ROS) affect the functionality of biological membranes by oxidation of unsaturated fatty acids (Critzer et al. 2007). ROS are supposed to have a dominating role in spore-killing over other factors such as UV light, heat, or charged particles (Deng et al. 2006). Hertwig et al. (2015b) inactivated bacterial spores with an indirect (remote) plasma, where only long half-life plasma species and no UV light contribute to the effect. The process gas is sucked by a vacuum pump from the plasma source in a container with the sample. The selectivity concerning inactivation principles in a remote plasma leads to an extended process time (e.g., 30 min) for obtaining relevant inactivation effects.

Out of the numerous forms of plasma-generating devices, those of high interest for the food industry provide plasma that can be applied at atmospheric pressure, or close to it. Direct exposure of food to the plasma is possible in a 1 atm uniform glow discharge plasma (Critzer et al. 2007; Kelly-Wintenberg et al. 1999), atmospheric plasma jets (Brandenburg et al. 2007; Reineke et al. 2015), or atmospheric DBD plasma (Butscher et al. 2016; Misra et al. 2014). Such types of plasma are not selective, meaning that all plasma species can potentially act on the sample. The peak voltage required for initiating a discharge and igniting the plasma depends on the gap width between plane electrodes of a DBD setup and the properties of a dielectric barrier covering one electrode (Fridman and Kennedy 2011; Roth 2001). Typically, the gap ranges from some millimeters with a peak voltage lower than 10 kV (Butscher et al. 2016) up to a gap of 40 mm for the treatment of fruits, for example, with a peak voltage of 120 or 60 kV (Misra et al. 2014). The plasma composition can be varied and controlled to a certain extent by encapsulating the electrodes and flushing the cell with a purified working gas.

The aims of the present study are (i) comparing inactivation kinetics of spores of *Bacillus subtilis*, *Bacillus coagulans*, *Geobacillus stearothermophilus*, and *Penicillium nalgiovense* exposed in a DBD setup, and (ii) elucidating influencing factors of the inactivation rate of *B. coagulans* spores in a powder matrix and thus contributing to an understanding of inactivation principles.

Materials and Methods

Microbial Strains and Preparation of Inoculum Subcultures

All isolates used in this study were obtained from the culture collection of wild strains of the HES-SO Valais-Wallis, Institute of Life Technologies (Sion, Switzerland). Spores of *Penicillium nalgiovense*, *Bacillus subtilis* subsp. *spizizenii*, *Bacillus coagulans*, and *Geobacillus stearothermophilus* were used as target microorganisms.

P. nalgiovense was transferred from stock cultures on malt agar (MEA, Biolife, Italy) and incubated for 5–7 days at 25 °C. The spores were harvested from the plates with 5 mL sterile peptone water (0.85% NaCl, 0.1% neutralized bacteriological peptone, 0.05% Tween 80) (Sigma Aldrich, Lausanne, Switzerland). The surface of the medium was scraped with a sterile glass spatula and the liquid phase was transferred to an Erlenmeyer flask containing 5 g of sterile glass balls. This suspension was centrifuged at 2000×*g* and 4 °C for 20 min. The pellet was re-suspended in sterile peptone water and centrifuged twice as described before to remove any remaining mycelium. The spore density was adjusted to approximately 10^7 spores/mL by dilution with 0.1% peptone water.

Bacterial endospores of *B. subtilis*, *B. coagulans*, and *G. stearothermophilus* were transferred from stock cultures on tryptic soy agar (TSA, Biolife, Italy) and incubated for 24 h at 37 °C (*B. subtilis*, *B. coagulans*) and 55 °C (*G. stearothermophilus*), respectively. After that, the strains were cultured in tryptic soy broth (TSB, Biolife, Italy) for 24 h with agitation at 150 rpm at appropriate temperatures (37 or 55 °C). The vegetative cells were harvested by centrifugation at 3000×*g* and 4 °C for 10 min and washed twice with sterile peptone water (0.85% NaCl and 0.1% neutralized bacteriological peptone) (Sigma Aldrich, Lausanne, Switzerland). The pellets were re-suspended in 0.1% peptone water. A volume of 600 μL of each spore suspension was layered onto TSA in 12 × 12 cm square versions of Petri dishes and incubated for 10 days at 37 or 55 °C, respectively. The appropriate sporulation was examined by contrast phase microscopy. Spores were harvested by depositing 10 mL sterile demineralized water (DMW) onto the surface of the culture plates and rubbing the upper layer using a sterile glass spatula. The spore suspensions were transferred to 50 mL tubes and heated in a water bath at 80 °C for 20 min to kill any vegetative cells. Heat-treated suspensions were then centrifuged at 450×*g* and 4 °C for 20 min. The pellet of each strain was re-suspended in sterile DMW. Afterward, 1% (v/v) lysozyme

was added. The tubes were shaken at 150 rpm for 30 s and stored overnight at − 20 °C. Spore suspensions were defrosted in a water bath at 25 °C and then centrifuged at 450×*g* and 4 °C for 20 min. The pellets were re-suspended and centrifuged as described before twice with sterile DMW and finally diluted to a concentration of approximately 10^7 spores/mL in sterile DMW. Routinely, spore dispersions were checked by phase-contrast microscopy for purity.

Inoculation and Sample Preparation

Spores were exposed to DBD plasma treatments on the sterile flat glass to compare the inactivation on this reference surface with two powder model-systems as a matrix: (i) diatomic earth, a highly porous material, and (ii) a food-grade rice starch with rather smooth particles. The samples were prepared as follows:

Reference surface: A volume of 1 mL of a spore suspension was spread evenly on the flat glass carriers (76 × 26 mm) and subsequently air-dried in a laminar flow cabinet overnight. The initial bacterial surface load equaled from 10^6 to 10^7 spores per glass carrier or approximately $5{\cdot}10^4$ to $5{\cdot}10^5$ spores per cm^2. The inactivation effect as a function of the initial surface load was assessed for *B. coagulans* from 10^4 to 10^7 spores per cm^2.

Powders as matrices: Suspensions of diatomic earth (Dicalite 215, Dicalite Management Group, Inc.) or rice starch (36–56 μm particle size) were prepared at 1 and 10% (w/v) concentration in sterile water. The suspensions were inoculated with *B. coagulans* spores to a final concentration of 10^8 CFU/mL. From this point on, the sample preparation protocol was identical to the preparation of the reference surfaces.

Plasma Source and Plasma Treatments

The experimental setup of the plasma device (type DBD: dielectric barrier discharge) is schematically illustrated in Fig. 1. The plasma discharge is generated between two water-cooled aluminum electrodes of 90 × 90 mm^2, separated by different dielectrics. The bottom grounded electrode is covered by a uniform Kapton® tape 65 μm thick, and a polypropylene sheet 100 μm thick with a hole in the middle of the size of the flat glass carrier (limitation to the effective part of the electrodes). With this arrangement, the discharges were concentrated above the entire flat glass, used as the spore carrier, which was placed into the hole with a 0.5-mm thin Al_2O_3 support. A gap of 3 mm to the upper alumina plate (Al_2O_3, 96%, 0.5 mm thickness) was maintained by Macor® spacers (Ceramic Substrates and Components Ltd., UK). The device was operated at atmospheric pressure using ambient air as working gas without active gas flow.

Electrical power was supplied by a function generator, a Titan™ Series (Compact Power Company, USA) low frequency power amplifier (45 Hz–15 kHz, max. power output 130 V/8 A or 1 kW), and a custom-designed high voltage transformer with 2–20 kHz bandwidth (Swiss Trafo Josef Betschart AG, Switzerland). The frequency was fixed at 10 kHz to ensure the optimal voltage gain of the transformer.

Testec HVP 15 HF (Testec Elektronik GmbH, Germany) and Sapphire HV 7000 APW6 70 MHz (Sapphire Instruments Co., Ltd., Taiwan) voltage probes and Pearson model 4100 and model 110 (Pearson Electronics, Inc., USA) current probes were used to measure the power input and output of the transformer with a 500-MHz Oscilloscope (Teledyne LeCroy, USA).

To calculate the discharge power, the current and the voltage responses were measured in the secondary circuit as a function of time.

The power is determined by the mean value over a period (T) of the current (I) multiplied by the voltage (U), an operation that is performed directly by the LeCroy oscilloscope:

$$P = \frac{1}{T}\int_0^T U(t) \times I(t)dt \quad (1)$$

Because the current (I) and the voltage (U) were measured at the secondary side of the transformer, Eq. (1) gives the total electrical power dissipated in the plasma reactor, which is the sum of the discharge power and the power dissipated in the electrode circuit, including the dielectrics: $P_{\text{total}} = P_{\text{discharge}} + P_{\text{circuit}}$. Since the DBD discharge current is represented by the current peaks, which are superposed on the sinusoidal current (Fig. 2), the sine component of the current trace was subtracted to obtain the DBD discharge current as a function of time. Equation (1) applied to this real discharge current trace gives the power consumed in the discharge. Note that

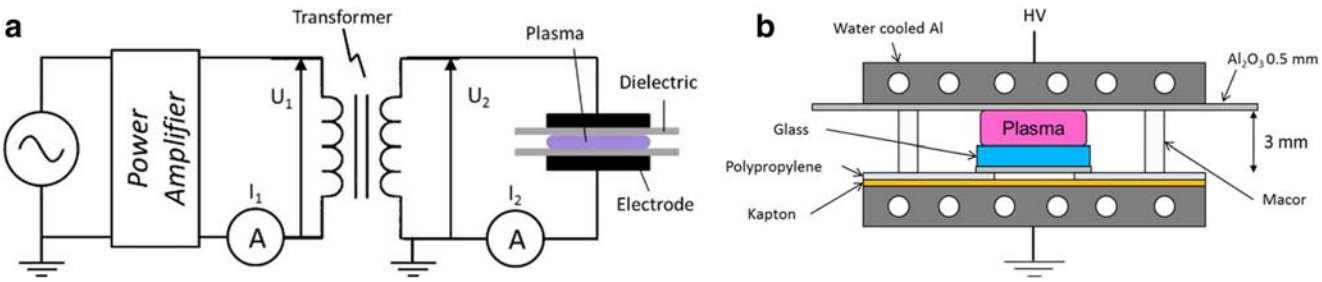

Fig. 1 DBD plasma device: electrical setup (left), and cross-section drawing showing the different dielectric barriers (right)

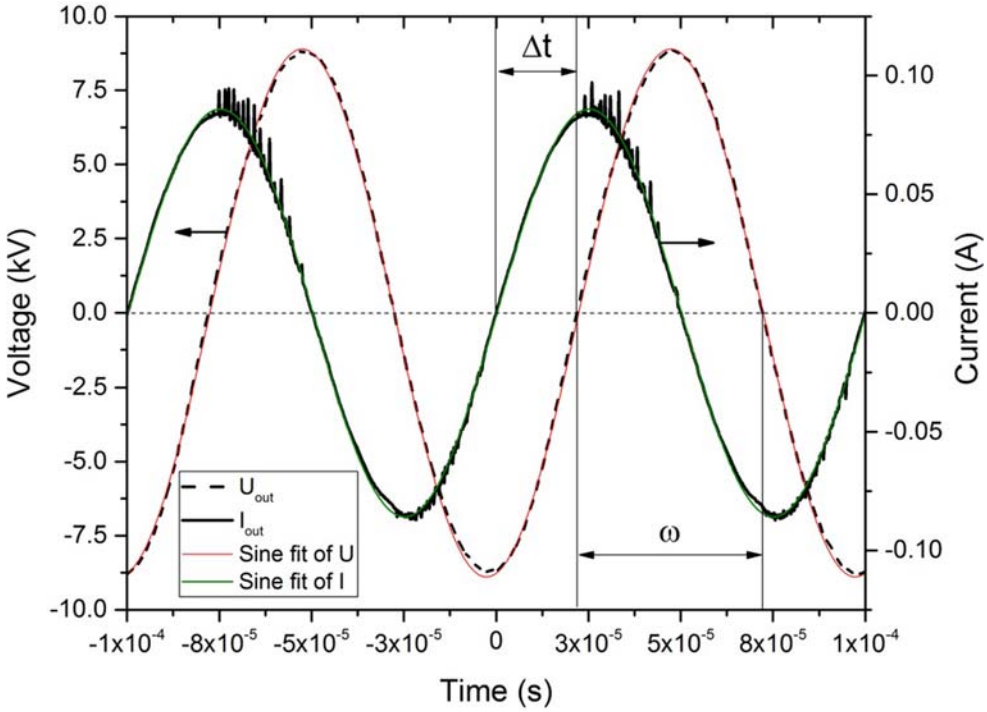

Fig. 2 Typical time traces of the secondary voltage U_2 and current I_2 in the DBD plasma. The spikes on the current curves represent the filamentary discharges occurring in the homogeneous plasma region

the total electrical power in our experiment is about 8 times larger than the power consumed in the discharge itself. While the discharge power is the relevant one to inactivate the spores, the total electrical power must be considered for the design of the plasma system to improve energy efficiency.

At a frequency of 10 kHz, the voltage amplitude oscillates, 10,000 times per second (see Fig. 2 as an example for 200 μs), and the plasma ignites within a few milliseconds. The ignition time can, therefore, be neglected to have any effects for treatment timescales of more than 1 s. Once the plasma is ignited, the measured intensity of excited radicals in the plasma is constant over the sequence of voltage oscillations.

The surface energy (E_{surface}) has the unit (J/cm^2) and is the product of the exposure time (t) and the discharge power ($P_{\text{discharge}}$) per unit electrode area ($A_{\text{electrode}}$):

$$E_{\text{surface}} = \frac{P_{\text{discharge}} \times t}{A_{\text{electrode}}} \quad (2)$$

The efficiency of the cooling system was tested by measuring the temperature inside the lower aluminum electrode using a K-type thermocouple (Thermocoax, France). For this purpose, the plasma device was operated at 10 kHz and 30 W (total electrical power) for 300 s. The temperature rise was determined once with the cooling system "on," and once when it was switched "off." It was found that the temperature rise of the electrodes was less than 5 and 19 °C with and without cooling, respectively. During a test, the average temperature, therefore, does not increase above 30 °C, when starting at room temperature.

For the optical emission spectroscopy, a UV light spectrometer (MayaPro 2000, Ocean Optics, USA) was used with a detection range of 200 to 425 nm and a wavelength resolution of 0.26 nm. A UV-grade optical fiber of 400 μm core diameter and 1 m length was installed at a fixed distance of 4 cm from the plasma.

To compare the effectiveness of the CAP treatment for various spore types, and elucidate the impact of the initial surface load with bacterial spores and powder particles, the surface energy ranged between 0 and 43 J/cm^2 ($P_{\text{discharge}}$ = 3.5 W, t < 240 s). For the assessment of *B. coagulans* spore inactivation as a function of discharge power (4.1, 5.7, and 7.1 W), the treatment time ranged between 0 and 20 s and, in conclusion, the surface energy was < 7.2 J/cm^2.

Inoculated glass carriers without plasma treatment were used as control samples and were noted as 0 s samples. Experiments were conducted at room temperature and each test was performed in triplicate.

Microbiological Analysis

Plasma-treated samples and also controls were transferred aseptically into 114 mm × 230 mm transparent sterile stomacher plastic bags (Carl Roth, Germany) immediately after the treatment. Ten milliliters of sterile 0.1% peptone water was added and the bags were sealed with the integrated wire. The samples were agitated by hand for 1 min then the glass carriers were removed using sterile tweezers. The spore dispersions were serially diluted with sterile water. *P. nalgiovense*

dispersion was plated (100 μL) on malt agar (MEA, Biolife, Italy) while *B. subtilis*, *B. coagulans*, and *G. stearothermophilus* dispersions were plated on TSA (Biolife, Italy). MEA plates were incubated at 25 °C for 5 days and TSA plates were incubated for 24 h at 37 °C (*B. subtilis*, *B. coagulans*) and 55 °C (*G. stearothermophilus*), respectively, before colonies counting. This procedure was performed in triplicate and microbiological counting of each replicate was done in duplicate.

Modeling the Inactivation Kinetics

The inactivation effect is the decimal logarithm of the ratio of the number of viable cells counted in suspension (2.4) before and after a DBD CAP treatment. For biphasic reactions, two distinct reaction constants k_1 and k_2 can be found.

$$\log_{10}\frac{N_t}{N_{o_1}} = -k_1 \times t = \frac{-t}{D_1} \quad \text{and} \quad \log_{10}\frac{N_t}{N_{0_2}} = -k_2 \times t = \frac{-t}{D_2} \tag{3a, b}$$

where $N_{0,1}$ and $N_{0,2}$ are the initial number of viable cells (CFU/mL) of the first and second phase of inactivation, t is the processing time (s) within the limits of a phase, and k_1 (s^{-1}) and k_2 (s^{-1}) are the reaction constants of the first and second phase of inactivation. The decimal reduction times, D_1 and D_2 (s), are then $1/k_1$ and $1/k_2$. The intersection of curves 3a and 3b marks the time limit separating the first from the second inactivation phase and the value of $N_{0,2}$.

All data were statistically analyzed (ANOVA) with Origin Pro 2015 (OriginLab Corporation, USA) to determine the significance (p value ≤ 0.05) influence of studied factors on inactivation as well as significant differences between CAP inactivation levels.

Results and Discussion

Comparative Resistance of *Bacillus* spp., *Geobacillus* spp., and *Penicillium* spp. Spores to the DBD CAP Treatment

Figure 3 displays the spore inactivation as a function of surface energy. In analogy to heat treatment and to deliver potentially comparable data, specific energy input (plasma power density), and the processing time are considered.

Inactivation kinetics was dominated by a fast inactivation, in the beginning, followed by slower inactivation or a saturation effect.

The obtained inactivation data were fitted by first-order kinetics according to Kelly-Wintenberg et al. (1999) and Moisan et al. (2013). Kelly-Wintenberg et al. (1999) suggested a decimal reduction time D_1 to indicate a "degree of basic susceptibility" of a given microorganism to the plasma's active species. Corresponding D_1 and D_2 values are presented in Table 1. In general, D_2 is larger than D_1, meaning that the initial inactivation rate is higher in the first phase compared to the second phase. The ratio of D_2 to D_1 varies from strain to strain between about 2 for *G. stearothermophilus* and 240 for *B. coagulans* (Table 1). Overlaying the two curves for each spore type, a bending point of the all-over behavior can be estimated to a value lower than 15 J/cm^2.

A biphasic inactivation behavior (Fig. 3) has been previously described by other authors regarding the spores' inactivation by plasma treatment on dry surfaces. Brandenburg et al. (2007), Hertwig et al. (2015a), and Reineke et al. (2015) explain that behavior by the involvement of different inactivation effects occurring under prolonged exposures or highly intensive treatments. The first inactivation stage might be attributed to (V)UV photons effect (Stapelmann et al. 2013). The slower inactivation of the second phase is thought to be associated to the decomposition of the spore through photodesorption and etching (Hertwig et al. 2017; Setlow 2006). However, the mechanisms responsible for bacterial spore inactivation remain incompletely understood (Deng et al. 2006; Hertwig et al. 2015a, 2017). Some influencers of the inactivation in a DBD plasma will be discussed after presenting data of plasma diagnostics in sections 3.2 and 3.3.

For spores, differences in composition and thickness of the exosporium, coats, cortex, and core of spores from different genera or even different strains belonging to the same genus are described and are supposed to be responsible for the different sensitivities to a given plasma exposure (Kim et al. 2014; Park et al. 2012; Setlow 2006).

***Bacillus* spp.** The most efficient inactivation was achieved with a 3.20 ± 0.09 $\log_{10}$ reduction for *B. coagulans* spores at surface energy of 3 J/cm^2, corresponding to treatment time of just 10 s. *B. subtilis* generates the most resistant spores amongst the studied spore-forming microorganisms (*Bacillus* spp., *Geobacillus* spp., and *Penicillum* spp.) with a maximum inactivation level close to 1 $\log_{10}$ cycle at surface energy of 20 J/cm^2.

Hertwig et al. (2017) found a similar D_1 value for *B. subtilis* spores exposed to a semi-direct surface barrier discharge plasma (350 W, 7 min, air) compared to the present study (1.22 versus 1.4 min, see Table 1). Also, Hertwig et al. (2017) compared DBD spores' resistance of a gene PS578-lacking strain to a wild-type strain and determined the higher resistance for the wild type strain. The PS578 gene encodes α/β-type SASPs (small, acid-soluble spore proteins). According to Hertwig et al. (2017), Reineke et al. (2015), and Setlow (2006), *B. subtilis* spore UV-resistance is largely due to an alteration in spore DNA photochemistry caused by binding

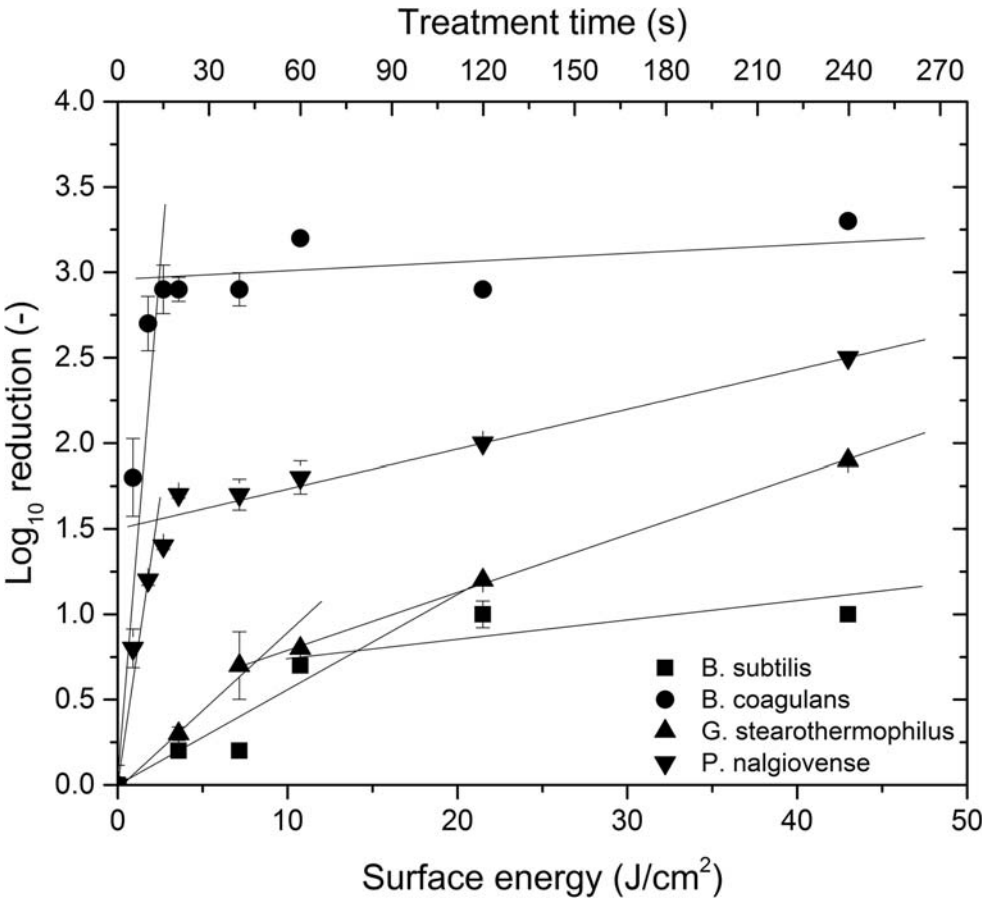

Fig. 3 Inactivation of spores at 3.5 W discharge power

of α/β-type SASPs to the DNA, and to a lesser extent to the photosensitizing action of the spore core's large pool of dipicolinic acid (DPA). Also, a characteristic spore photoproduct (SP, a thymidyl-thymidine adduct) has been previously described by Douki et al. (2005). However, SP is repaired in the first minutes of spore outgrowth by a SP lyase (Setlow 2006). The higher resistance of *B. subtilis* spores compared to *B. coagulans* spores is related to one of the mentioned factors, most probably the potential of formation of SASPs.

***Geobacillus* spp. and *Penicillium* spp.** In the present study, a maximum inactivation level of 1.60 ± 0.02 $\log_{10}$ cycles was achieved for *G. stearothermophilus* after 240 s of DBD plasma exposure, or at surface energy of 22 J/cm^2 and a frequency of 10 kHz. Morris et al. (2009) required 15 min to achieve 0.5 $\log_{10}$ cycles of *G. stearothermophilus* inactivation (DBD plasma, 60 Hz, 9 kV) and Akitsu et al. (2005) required 3 min for a ≥ 3 $\log_{10}$ cycles inactivation (DBD plasma, 13.56 MHz; cellulose matrix). The results are not directly comparable, as the surface energy was not calculated in all cases. However, comparing the studies on *Geobacillus*, it can be inferred that the higher the frequency and the processing time, the higher the inactivation effect.

Comparing the sensitivity of endospores of *G. stearothermophilus* and *B. subtilis* directly, Klämpfl et al. (2012) reported similar average rates of inactivation for both strains as found in the present study. However, the final $\log_{10}$-reduction was a factor 2.5 higher for *G. stearothermophilus*, when inactivating the endospores with a semi-direct plasma type (Klämpfl et al. 2012).

Table 1 Decimal reduction times (D values) for microbial spores for a DBD plasma treatment with a discharge power of 3.5 W

Type of spores	$\log_{10}$ of initial number [−]	$\log_{10}$ reductions by DBD CAP [−]	D_1 value [min]	D_2 value [min]
B. coagulans	6.5	3.3	0.1	23.8
P. nalgiovense	6.0	2.5	0.2	4.5
G. stearothermophilus	6.2	1.9	1.1	2.5
B. subtilis	7.2	1.0	1.4	4.9

In general, information on the sensitivity of spores of fungi to plasma are scarce and focused on decontamination of seeds, nuts, and powdered food (Butscher et al. 2016; Kim et al. 2014; Iseki et al. 2010). A maximum of 2.30 $\log_{10}$ cycles of inactivation was achieved for *P. nalgiovense* spores under the studied conditions (e.g., 43 J/cm^2 or 3.5 W/cm^2, 300 s). According to the studies of Selcuk et al. (2008), a maximum reduction of 3 $\log_{10}$ cycles of *Penicillum* spp. spores could be achieved in seeds and legumes, using low pressure, air or hexafluoride plasma at a power input of 300 W and an exposure time of 15 min.

Scaling Inactivation Effects Through the Discharge Power and Inactivation Principles

Theoretically, the inactivation effect relates to the surface energy in DBD CAP treatments and can be controlled not only by process time but also by discharge power variation. For verification of this concept, the discharge power was set to 4.1, 5.7, and 7.1 W for a processing time up to 20 s.

The initial inactivation rate for *B. coagulans* spores depended significantly (p value ≤ 0.05) on the discharge power applied (data not plotted). The higher the discharge power, the higher the inactivation rate achieved within the first 5 s of treatment. Represented in a surface energy–inactivation effect plot, for different discharge power a single inactivation curve appears for the first and second phases of inactivation. At surface energy higher than approximately 1.5 J/cm^2, a saturation effect close to 2 $\log_{10}$ cycles can be observed (Fig. 4).

Based on these observations, the inactivation constant k_2 is assumed to be next to 0 s^{-1} (see Table 1). At least, in technologically feasible process times, the final bacterial cell count (N_{infinit}) is larger than 0 CFU/mL. In the specific case, we estimate N_{infinit} to be about 1.2×10^5 CFU/mL. This value characterizes under these treatment conditions immortal spores, including spores, which are non-ideally exposed to the plasma. The fit curve as presented in Fig. 4 is based upon Eqs. 4 and 5:

$$N_t = N_{0_1} \times 10^{-k_1 \times t} + N_{0_2} \times 10^{-k_2 \times t} \quad (4)$$

For $k_2 = 0$ and by replacing the processing time (t) with the universal parameter "surface energy" (E_{surface}), follows Eq. (5):

$$N_{E_{\text{surface}}} = N_{0_1} \times 10^{-k_1 \times E_{\text{surface}}} + N_{\text{infinit}} \quad (5)$$

The unit of k_1 in Eq. (5) is (cm^2/J).

To investigate the relation discharge power and plasma density, optical emission spectra (OES) were recorded during the spore treatment. Over the studied discharge power input range, the intensity of all nitrogen bands increased linearly (Fig. 5, the inset shows a typical spectrum in the UV range). OES lines characteristic for excited oxygen species have not been observed (Fig. 5). In conclusion, the concentration of oxygen radicals is estimated to be low likewise. However, the increase is less than 10% of the intensity at the lowest discharge power input. According to Zhu and Pu (2005), the emission band intensities of excited nitrogen molecules $I(N_2^*)$ and the density of nitrogen radicals $n(N_2^{\bullet})$ depend nearly linearly on the electron density. Generally, the plasma density n_e is thought to be proportional to the discharge power (Lieberman and Lichtenberg 2005). Therefore, taken alone, the UV light intensity increase of about 10% with the total power input increase does not explain the increase in the initial rate of inactivation k_1.

The relatively weak increase of the OES-intensity with total power is suggested to go along with a non-linear increase of the kinetic energy of ions. Babaeva et al. (2012) have described earlier already a positive correlation of kinetic energy of ions and destructive effects on lipid-like surfaces. In general, the kinetic energy of charged particles increases in the square with the electric field strength. This delivers the argument for the amplifier effect of plasma power increments on the inactivation of spores. The observation enables conclusions on inactivation principles.

The photo-oxidation (1st principle) of the coat of endospores is considered to be triggered by UV radiation (200–400 nm). The detected intensity of UV-A and UV-B increases slightly with the plasma power (Fig. 5), and is supposed to contribute to inactivation effects, but do not explain non-linear, overproportioned inactivation effects with increasing plasma power.

Reactive oxygen or/and nitrogen species (ROS, RNS) trigger etching (2nd principle) or "atom by atom erosion" of the protein coat and the peptidoglycan cortex (Deng et al. 2006; Van Bokhorst-van de Veen et al. 2015). In consequence, the hull's permeability increases. Erosion is supposed to be a function of RNS concentration (Fig. 5) and the kinetic energy of charged particles. This delivers an explanation for observed inactivation kinetics.

Subsequently, ROS and RNS might diffuse into spores (3rd principle) and alter the cytoplasmic membrane, metabolic proteins, and DNA irreversibly. It will be shown in the following paragraph that the rate of diffusion outside and inside of spores is low and does not exceed the effect of erosion.

Spore Surface Load and Powder Matrix: Modification of the Inactivation Efficiency for *B. coagulans*

B. coagulans spores were selected to elucidate the influence of the spore load on flat glass carriers on the efficiency of the inactivation by a DBD CAP. Theoretically, a monolayer of spores will be formed by 5×10^7 spores per cm^2 or 10^9 *B. coagulans* spores per carrier flat glass (surface area = 19.8 cm^2). The monolayer load was calculated according to a model by Deng et al. (2005).

According to the obtained results, applying surface energy of 1.8 J/cm^2 and for surface loads between 10^4 and 10^5 spores

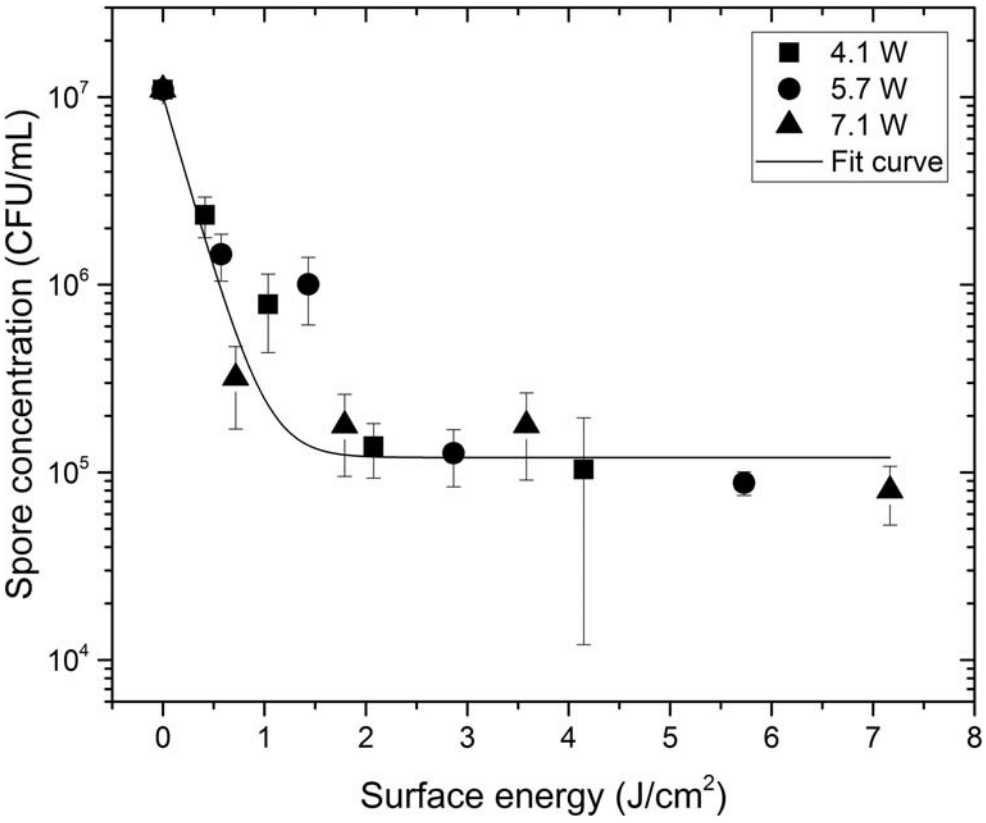

Fig. 4 Concentration of *B. coagulans* spores as a function of the surface energy. The discharge power varied from 4.1 to 7.1 W and the maximal exposure time was 300 s. The fitting curve is related to Eq. (5)

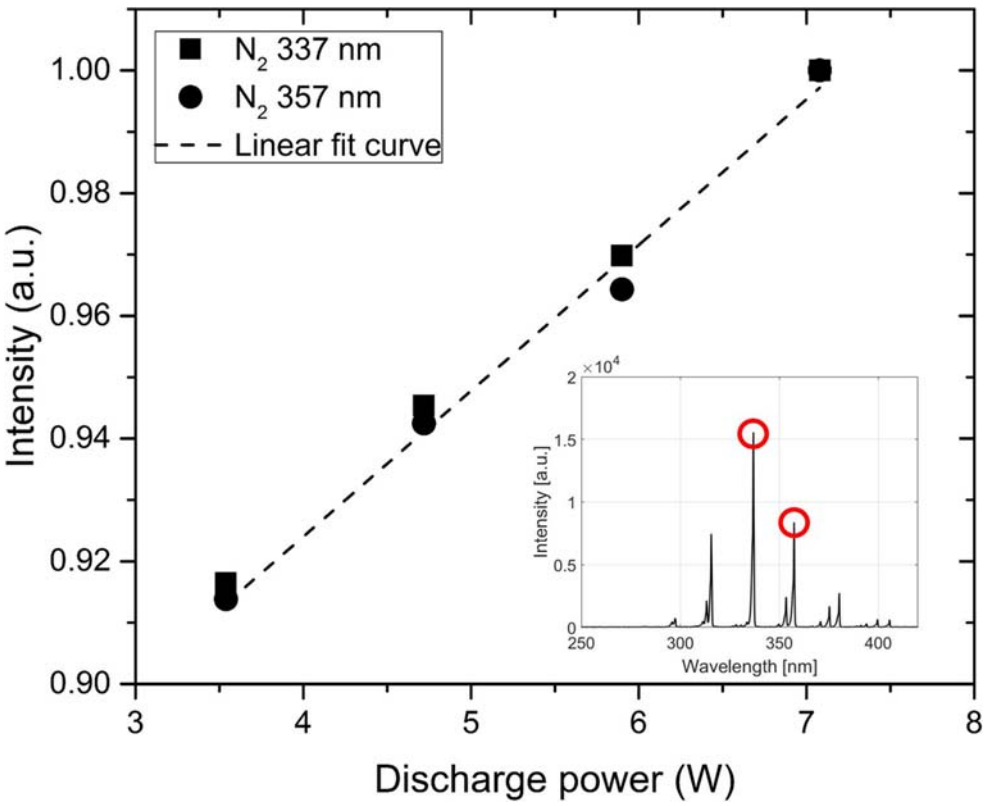

Fig. 5 Increase of two N_2 emission bands intensity as a function of the discharge power. Inset: typical OES spectrum in the UV range of 200–425 nm

per cm^2, a reduction of close to 1.6 ± 0.5 log_{10} cycles was achieved. At higher initial surface loads of 10^6 and 10^7 spores per cm^2, a reduction of close to 2.5 ± 0.5 log_{10} cycles was detected. A surface loaded up to the monolayer limit is not restricting the inactivation efficiency. The higher inactivation efficiency at a higher spore surface load might be justified by a reaction rate that is limited by low concentrations of spores. The concentration of reactive plasma species is reasoned to be not a limiting factor in this setup.

For testing the impact of powdered matrices on the inactivation of *B. coagulans* spores by a DBD CAP, the spore suspensions were not spread directly on flat glass carriers (reference model) but mixed in the aqueous phase with a non-soluble powder, subsequently spread on flat glass carriers, dried, and finally exposed to the plasma. A surface energy of 11 or 22 J/cm^2 was applied.

The inactivation effect for spores directly exposed to DBD CAP on the flat glass carriers (reference value) was clearly reduced by native rice starch granules (non-porous powder model system) and even more, reduced by shells of diatoms (highly porous powder model system) (Fig. 6).

The concentration of the starch was 1 or 10% (w/v) in the initial suspension, meaning with 1 mL of the suspension 0.5 or 5.0 mg of starch granules/cm^2 was deposited on the glass carriers in a mixture with *B. coagulans* spores. The higher the starch surface load, the lower the inactivation achieved. Granules are related to significant protective effects, most probably shadowing of UV light (Deng et al. 2006; Hertwig et al. 2015a, b, 2017; Reineke et al. 2015) and structural modification of starch (Chen 2014; Chen et al. 2015; Muhammad et al. 2018) and zein powder (Dong et al. 2017) by plasma has been previously described. An alternative explanation is based on the erosion effect on particles in general and spores specifically. As already discussed (3.2), ions will be accelerated in an electric field and a bombardment with ions has to be supposed. Shielding of spores from this bombardment is possible by larger particles at a relatively high surface load. In contrast, the surface load with contaminated particles does not change the diffusion length of the plasma species to the surface of the particles. The concentration of plasma species is supposed to be homogenous between the electrodes.

In the present study, while native starch granules are characterized by a smooth surface, the shells of diatoms are very porous. Diatomic earth is used for this property in deep bed filtration. Independently of the amount of diatomic earth deposited on the glass carriers, the inactivation effect is reduced by the same magnitude (Fig. 6). Spores that are hidden largely from the erosion effect and UV light by the porous calcium carbonate structure, even at the lower surface load of the powder. In contrast, spores that are deposited on the outer surface of starch granules are accessible for erosion factors to a higher extent.

The diffusion rate and the half-life of RS do not enable efficient transport toward the deposition spot of the spores inside of the porous diatom shells. According to the research work of Hertwig et al. (2015b), *B. subtilis* spore inactivation

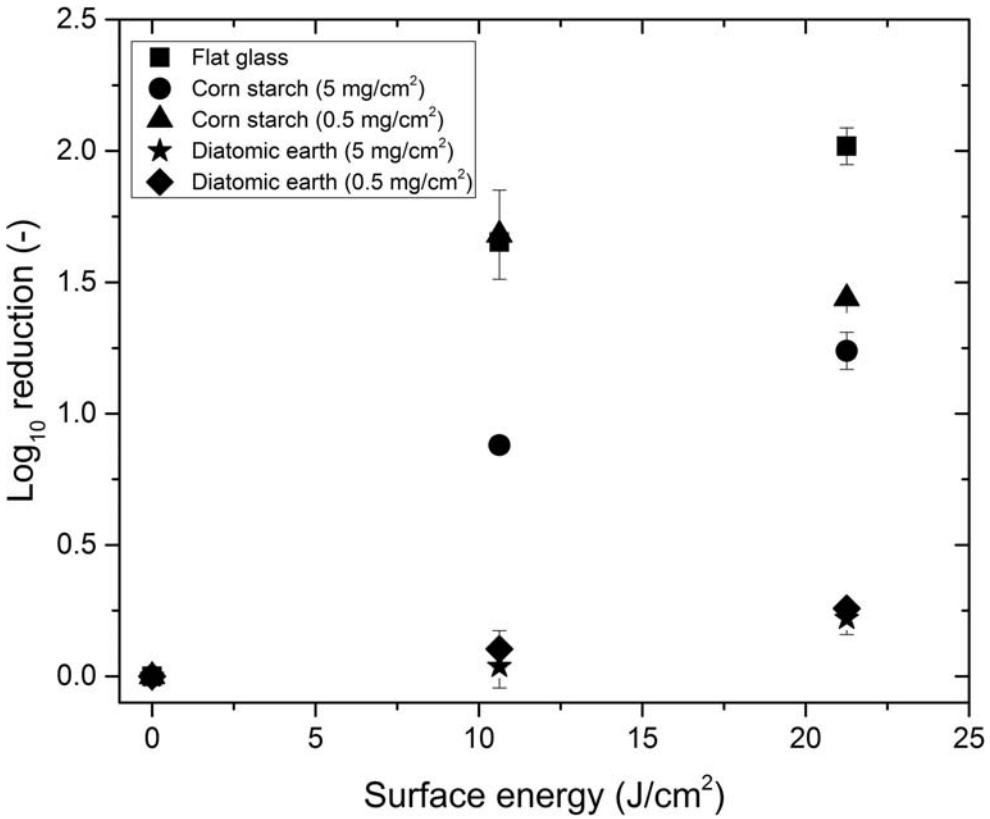

Fig. 6 Decimal logarithm reduction (log_{10} [N/N_0]) of *B. coagulans* spores disposed directly on flat glass, contaminated native corn starch (0.5 or 5 mg/cm^2), or contaminated diatomic earth (0.5 or 5 mg/cm^2). DBD CAP conditions: 3.5 W discharge power

levels in peppercorns resulted in the lowest inactivation (less than 1.0 $\log_{10}$ after 15 min) compared to planar glass Petri dishes and glass beads applying the same plasma conditions. Such examples illustrate the importance of matrix structure effects in CAP treatments for the inactivation of microbial spores. A detailed description of the porosity and chemical nature of a matrix would be required for a dose-effect quantification and classification of shielding materials.

Butscher et al. (2016) applied a vibrating table to fluidize and expose polypropylene beads and wheat grains more evenly during the plasma treatment. The microstructure of wheat grains is considered the reason for a 4 $\log_{10}$ cycle lower inactivation of *G. stearothermophilus* endospore compared to an exposition on plastic beds and within a 10-min exposition period to a DBD plasma. However, compared the results of the present study (2.5 $\log_{10}$ cycles inactivation for *G. stearothermophilus* in 5 min), the vibrating table used by Butscher et al. (2016) might be responsible for the slightly higher inactivation efficiency (3 $\log_{10}$ cycles within 4 min).

Conclusions

Only very low surface energy is required to achieve effective spore inactivation (≈ 3 $\log_{10}$ cycles for *B. coagulans*) by a DBD plasma setup and with ambient air as the process gas. Spores of *B. subtilis* are the most resistant amongst the studied strains (D_1 = 1.4 min). A higher rate of inactivation in the first seconds of exposition is followed by a low rate, a pattern, which is pronounced for *B. coagulans* endospores. A new model considering this pattern in addition to the determining impact of the surface energy was proposed. The short process time is advantageous in scaling toward a large-scale application. The process might run at ambient pressure and in air. Amongst different inactivation principles, the most evident is the erosion of spores' coat triggered by reactive nitrogen species, and charged species specifically, that are transported efficiently to the spores' surface by increments of the electric field strength. UV radiation might contribute to the inactivation effect but is supposed to be a second-order factor as long the spores' coat protects the genetic material. Cavities in shells of diatoms shield microorganisms a magnitude better than starch particles with smooth surfaces. This demonstrates the structure effect. Increasing the efficiency of this decontamination method would require a higher plasma power and fluidized bed technology. However, a limitation of the inactivation potential is still given by shielding effects in porous materials.

Funding Information This research was funded by the Sciex-NMS^{ch} Program (Swiss Confederation) under the project code 13.149, the University of Applied Sciences and Arts Western Switzerland in the frame of the thematic program "HealthFood" under the project code 39237, and the EC with an MSCA-IF grant under the code 748314.

Compliance with Ethical Standards

Conflict of Interest The authors declare that they have no conflict of interest.

Ethics Requirements This article does not contain any studies with human or animal subjects.

References

Akitsu, T., Ohkawa, H., Tsuji, M., Kimura, H., & Kogoma, M. (2005). Plasma sterilization using glow discharge at atmospheric pressure. *Surface and Coatings Technology, 193*(1–3), 29–34.

Babaeva, N. Y., Ning, N., Graves, D. B., & Kushner, M. J. (2012). Ion activation energy delivered to wounds by atmospheric pressure dielectric-barrier discharges: sputtering of lipid-like surfaces. *Journal of Physics D: Applied Physics, 45*, 1–12.

Black, E. P., Setlow, P., Hocking, A. D., Stewart, C. M., Kelly, A. L., & Hoover, D. G. (2007). Response of spores to high-pressure processing. *Comprehensive Reviews in Food Science and Food Safety, 6*(4), 103–119.

Brandenburg, R., Ehlbeck, J., Stieber, M., Woedtke, T. V., Zeymer, J., & Schlüter, O. (2007). Antimicrobial treatment of heat sensitive materials by means of atmospheric pressure rf-driven plasma jet. *Contributions on Plasma Physics, 47*(1–2), 72–79.

Butscher, D., Zimmermann, D., Schuppler, M., & von Rohr, P. R. (2016). Plasma inactivation of bacterial endospores on wheat grains and polymeric model substrates in a dielectric barrier discharge. *Food Control, 60*, 636–645.

CDC (Centers for Disease Control and Prevention) (2014). Multistate outbreak of *Salmonella* infections linked to organic sprouted chia powder (final update). Available at: http://www.cdc.gov/salmonella/newport-05-14/index.html /Accessed 27.07.15.

Chen, H. H. (2014). Investigation of properties of long-grain brown rice treated by low-pressure plasma. *Food and Bioprocess Technology, 7*(9), 2484–2491.

Chen, H. H., Hung, C. L., Lin, S. Y., & Liou, G. J. (2015). Effect of low-pressure plasma exposure on the storage characteristics of brown rice. *Food and Bioprocess Technology, 8*, 471–477.

Cheon, H. L., Shin, J. Y., Park, K. H., Chung, M. S., & Kang, D. H. (2015). Inactivation of foodborne pathogens in powdered red pepper (*Capsicum annuum* L.) using combined UV-C irradiation and mild heat treatment. *Food Control, 50*, 441–445.

Critzer, F. J., Kelly-Wintenberg, K., South, S. L., & Golden, D. A. (2007). Atmospheric plasma inactivation of foodborne pathogens on fresh produce surface. *Journal of Food Protection, 70*(10), 2290–2296.

Deng, X. T., Shi, J. J., Shama, G., & Kong, M. G. (2005). Effects of microbial loading and sporulation temperature on atmospheric

plasma inactivation of *Bacillus subtilis* spores. *Applied Physics Letters, 87*, 1–2.

Deng, X., Shi, J., & Kong, M. G. (2006). Physical mechanism of inactivation of *Bacillus subtilis* spores using cold atmospheric plasmas. *IEEE Transactions on Plasma Science, 34*(4), 1310–1316.

Dobrynin, D., Fridman, G., Fridman, G., & Fidman, A. (2009). Physical and biological mechanisms of direct plasma interaction with living tissue. *New Journal of Physics, 11*, 1–26.

Dong, S., Gao, A., Xu, H., & Chen, Y. (2017). Effects of dielectric barrier discharges (DBD) cold plasma treatment on physicochemical and structural properties of zein powders. *Food and Bioprocess Technology, 10*, 434–444.

Douki, T., Setlow, B., & Setlow, P. (2005). Effects of the binding of alpha/beta-type small, acid-soluble spore proteins on the photochemistry of DNA in spores of *Bacillus subtilis* and in vitro. *Journal of Photochemistry and Photobiology, 81*(1), 163–169.

Fridman, A., & Kennedy, L. (2011). In Taylor & Francis (Ed.), *Plasma physics and engineering* (2nd ed., p. 576). London: CRC Press.

Gurol, C., Ekinci, F. Y., Aslan, N., & Korachi, M. (2012). Low temperature plasma for decontamination of *E. coli* in milk. *International Journal of Food Microbiology, 157*, 1–5.

Hertwig, C., Reineke, K., Ehlbeck, J., Erdogdu, B., Rauh, C., & Schlüter, O. (2015a). Impact of remote plasma treatment on natural microbial load and quality parameters of selected herbs and spices. *Journal of Food Engineering, 167*, 12–17.

Hertwig, C., Steins, V., Reineke, K., Rademacher, A., Klocke, M., Rauh, C., & Schlüter, O. (2015b). Impact of surface structure and feed gas composition on *Bacillus subtilis* endospore inactivation during direct plasma treatment. *Frontiers in Microbiology, 6*(774), 1–12.

Hertwig, C., Reineke, K., Rauh, C., & Schlüter, O. (2017). Factors involved in *Bacillus* spore's resistance to cold atmospheric pressure plasma. *Innovative Food Science and Emerging Technologies, 43*, 173–181.

Hörmannsperger, J. T., Buchmann, L., Merz, S., Schmitt, R., Beyrer, M., & Windhab, E. J. (2016). Microbial decontamination of porous model food powders by vacuum-steam-vacuum treatment. *Innovative Food Science and Emerging Technologies, 34*, 367–375.

Iseki, S., Ohta, T., Aomatsu, A., Ito, M., Kano, H., Higashijima, Y., & Hori, M. (2010). Rapid inactivation of *Penicillium digitatum* spores using high-density nonequilibrium atmospheric pressure plasma. *Applied Physics Letters, 96*(15), 1–3.

Jung, K., Song, B. S., Kim, M. J., Moon, B. G., Go, S. M., & Kim, J. K. (2015). Effect of X-ray, and electron beam irradiation on the hygienic and physicochemical qualities of red pepper powder. *LWT–Food Science and Technology, 63*, 846–851.

Kelly-Wintenberg, K., Hodge, A., Montie, T. C., Deleanu, L., Sherman, D., & Roth, J. R. (1999). Use of a one-atmosphere uniform glow discharge plasma to kill a broad spectrum of microorganisms. *Journal of Vacuum Science and Technology A, 17*(4), 1539–1544.

Kim, J. E., Lee, D. U., & Min, S. (2014). Microbial decontamination of red pepper powder by cold plasma. *Food Microbiology, 38*, 128–136.

Klämpfl, T. G., Isbary, G., Shimizu, T., Li, Y. F., Zimmermann, J. L., Stolz, W., Schlegel, J., Morfill, G. E., & Schmidt, H. U. (2012). Cold atmospheric air plasma sterilization against spores and other microorganisms of clinical interest. *Applied and Environmental Microbiology, 78*(15), 5077–5082.

Kozempel, M., Radewonuk, E. R., Scullen, O. J., & Golberg, N. (2002). Application of the vacuum/steam/vacuum surface intervention process to reduce bacteria on the surface of fruit and vegetables. *Innovative Food Science and Emerging Technologies, 3*, 63–72.

Lieberman, M. A., & Lichtenberg, A. J. (2005). *Principles of plasma discharges and materials processing* (2nd ed.pp. 334–338). Hoboken: John Wiley & Sons.

Misra, N. N., Patil, S., Moiseev, T., Bourke, P., Mosnier, J. P., Keener, K. M., & Cullen, P. J. (2014). In-package atmospheric pressure cold plasma treatment of strawberries. *Journal of Food Engineering, 125*, 131–138.

Mitra, A., Li, Y.-F., Kämpfl, T. G., Shimizu, T., Jeon, J., Morfill, G. E., & Zimmermann, J. L. (2014). Inactivation of surface-borne microorganisms and increased germination of seed specimen by cold atmospheric plasma. *Food Bioprocess Technology, 7*, 645–653.

Moisan, M., Boudam, K., Carignan, D., Kéroack, D., Levif, P., Barbeau, J., Séguin, J., Kutasi, K., Elmoualij, B., Thellin, O., & Zorzi, W. (2013). Sterilization/disinfection of medical devices using plasma: the flowing afterglow of the reduced-pressure N_2-O_2 discharge as the inactivating medium. *European Physics Journal Applied Physics, 63*, 1–46.

Morris, A. D., McCombs, G. B., Akan, T., Hynes, W., Laroussi, M., & Tolle, S. L. (2009). Cold plasma technology: bactericidal effects on *Geobacillus stearothermophilus* and *Bacillus cereus* microorganisms. *Journal of Dental Hygiene, 83*(2), 55–61.

Muhammad, A. I., Xiang, O., Liao, X., Liu, D., & Ding, T. (2018). Understanding the impact of nonthermal plasma on food constituents and microstructure—a review. *Food and Bioprocess Technology, 11*, 463–486.

Muranyi, P., Wunderlich, J., & Heise, M. (2008). Influence of relative gas humidity on the inactivation efficiency of a low temperature gas plasma. *Journal of Applied Microbiology, 104*(6), 1659–1666.

Park, G., Ryu, Y. H., Hong, Y. J., Choi, E. H., & Uhm, H. S. (2012). Cellular and molecular responses of *Neurospora crassa* to nonthermal plasma at atmospheric pressure. *Applied Physics Letters*. https://doi.org/10.1063/1.3684632.

Reineke, K., Langer, K., Hertwig, C., Ehlbeck, J., & Schlüter, O. (2015). The impact of different process gas compositions on the inactivation effect of an atmospheric pressure plasma jet on *Bacillus* spores. *Innovative Food Science and Emerging Technologies, 30*, 112–118.

Riesenman, P. J., & Nicholson, W. L. (2000). Role of the coat layers in *Bacillus subtilis* spore resistance to hydrogen peroxide, artificial UV-C, UV-B, and solar UV radiation. *Applied and Environmental Microbiology, 66*(2), 620–626.

Roth, J. R. (2001). *Industrial plasma engineering: volume II—applications to nonthermal plasma processing* (p. 656). Bristol: Institute of Physics Publishing.

Selcuk, M., Oksuz, L., & Basaran, P. (2008). Decontamination of grains and legumes infected with *Aspergillus* spp. and *Penicillum* spp. by cold plasma treatment. *Bioresources Technology, 99*, 5104–5109.

Setlow, P. (2006). Spores of *Bacillus subtilis*: their resistance to and killing by radiation, heat and chemicals. *Journal of Applied Microbiology, 101*(3), 514–525.

Stapelmann, K., Fiebrandt, M., Raguse, M., Awakowicz, P., Reitz, G., & Moeller, R. (2013). Utilization of low-pressure plasma to inactivate bacterial spores on stainless steel screws. *Astrobiology, 13*(7), 597–606.

van Bokhorst-van de Veen, H., Xie, H., Esveld, E., Abee, T., Mastwijk, H., & Groot, M. N. (2015). Inactivation of chemical and heat-resistant spores of *Bacillus* and *Geobacillus* by nitrogen cold atmospheric plasma evokes distinct changes in morphology and integrity of spores. *Food Microbiology, 45*, 26–33.

Wang, J., Zhuang, H., & Zhang, J. (2016a). Inactivation of spoilage bacteria in package by dielectric barrier discharge atmospheric cold plasma—treatment time effects. *Food and Bioprocess Technology, 9*, 1648–1652.

Wang, S., Doona, C. J., Setlow, P., & Li, Y. Q. (2016b). Characterization of cold atmospheric plasma inactivation of individual bacterial spores using Raman spectroscopy and phase contrast microscopy. *Applied and Environmental Microbiology*. https://aem.asm.org/content/82/19/5775.

Zhu, X. M., & Pu, Y. K. (2005). Determining the electron temperature in inductively coupled nitrogen plasmas by optical emission spectroscopy with molecular kinetic effects. *Physics of Plasmas*. https://doi.org/10.1063/1.2061587.